Int. J. Electrochem. Sci., 12 **(2017)** 9320 – 9334, doi: 10.20964/2017.10.61

International Journal of
ELECTROCHEMICAL
SCIENCE
www.electrochemsci.org

Facile Synthesis of Polypyrrole Nanotubes and Their Supercapacitive Application

Yan Yan†[1,2], Huiqin Li†[1,2], Yuan Zhang[1,2], Jinqing Kan[1,2], Tengfei Jiang[1,2], Huan Pang[1,2,] Zhengxi Zhu[1,2,*] and Huaiguo Xue[1,2,*]*

[1] School of Chemistry and Chemical Engineering, Yangzhou University, Yangzhou, 225002, Jiangsu, P. R. China.
[2] Institute for Innovative Materials and Energy, Yangzhou University, Yangzhou, 225002, Jiangsu, P. R. China.
† These authors contributed equally to this paper.
[*]E-mail: huanpangchem@hotmail.com; zhuzx@yzu.edu.cn; chhgxue@yzu.edu.cn;

Received: 20 June 2017 / *Accepted:* 7 August 2017 / *Published:* 12 September 2017

Polypyrrole nanotubes (PPy-NTs) with uniform diameters were synthesized by the situ chemical oxidation polymerization with pyrrole, methyl orange (MO) and $FeCl_3$ as material, dopant and oxidant, respectively. The products were characterized by TEM, SEM, IR, EDS and TGA. polymerization parameters, such as the concentrations of reactants, temperature, and the types of solvents on the diameters of the nanotubes have been investigated. The results showed that the diameters of the PPy-NTs can be controlled in a relatively stable value (~100 nm) by adjusting the concentrations of reactants, temperature, types of solvents. The diameter of PPy-NTs affect the capacitive behavior of active material. The maximum specific capacitance is 960 F g^{-1} at 0.5 A g^{-1} with the concentrations of $FeCl_3$, MO and Py are 250 mM, 5.0 mM, and 50.0 mM, respectively. It also shows excellent cycle performance, after 10000 charge and discharge cycle the specific capacitance was still maintained as the original 97.1%. This study basically provides a new method for controlling the composition of PPy-NTs with uniform diameter, which facilitates the development of electrochemically active materials for supercapacitors.

Keywords: polypyrrole, nanotubes; supercapacitor

1. INTRODUCTION

The supercapacitors, also call electrochemical capacitors or ultracapacitors, are a novel energy storage device. Supercapacitors not only have the capability rapid store but also have efficiently delivered electric energy. Compared with other batters, supercapacitors have a lot of advantages such as high power density, long operational life and low maintenance cost. In recent years, electrochemical capacitor is a popular energy storage device composed with electrode materials such as carbon materials, transition metal oxide and conducting polymer [1-6].

Since Shirakawa et al [7-10] discovered that polyacetylene could reach extremely high conductivities, the polymer materials have no longer been regarded as electrical insulators. Subsequently, the discovery of polyaniline [11, 12], polypyrrole [13, 14], poly (thiophene) [15] expanded the type of conductive polymers [10]. The conductive polymers were employed in chemical sensors, solar cells [16], energy storage [17-20] and other applications [21].

Conducting polymers have been widely investigated for electronic, electrochemical and optical applications due to its unique chemical, electrical and optical properties. With appropriate elements doping, conductivity of the products can be varied from semiconductor to metallic regime [22]. Various templates have been used to synthesis polymer nanotubes for the electrochemical and chemical reactions methods [13, 23-27]. Electrochemical method had many disadvantages because of its harsh conditions and complex process [28, 29]. There were two chemical methods to prepare conducting polymer nanostructures [30]: hard template method and template-free method. The former method is that the conducting polymers are synthesized with solid inorganic membranes or fibers [31-33], such as porous alumina film, which is tedious to dissolve and also may destroy the structures of the resulting materials [28, 34, 35]. Therefore, to obtain aligned microstructures with the morphology desired without using a template, which has been a challenge at present. Template-free method employs super molecular assemblies of auxiliary organic substances, such as surfactant micelles [34, 36] or aggregates of dyes [37] as structure-guiding agents [24, 38, 39], which is proposed to grow conducting polymer in a tubular structure and needn't be treat by high temperature, strong acid, strong alkali to remove after the polymerization [24, 28, 40]. The template-free method above has become a versatile and effective method to synthesize conducting polymer nanotubes.

Among the family of conducting polymers, PPy has been the most extensively investigated due to its electrical properties, environmental stability and that they could be modified by changing the oxidations and protonation. PPy has an aromatic ring and a π-conjugated structure. PPy micro/nanotubes have potential applications in chemical sensors, super capacitor, biosensors, actuators and dye-sensitized solar cells [41] were reported on template-free synthesis of PPy micro/nanotubes, in which the dopant of MO was used. Yang et al [24] successfully synthesized PPy nanotubes via a facile self-assembly process by adding MO, which could direct the growth of PPy nanotubes, and was automatically eliminated during the preparation process [29]. The method of PPy nanotubes synthesized by Navarchian [29] was similar to that by Yang, and the MO-iron (III) chloride ($FeCl_3$) were considered as the fibrillary template. However, a defined synthesis mechanism of PPy nanotube by using MO hasn't been proposed up to now. Better understanding on the formation mechanism is benefit to controlling the diameter of PPy nanotubes and increasing their yield.

PPy-NTs with different nanostructures and morphologies become appropriate electrode materials for super capacitor because of low cost, easy synthesis method, and relatively high conductivity.

In the present work, PPy nanostructures were prepared with MO as a dopant at varying reaction conditions. The MO generated circular vesicles and stack together due to π-π interaction, in which the pyrrole monomer polymerized and grew simultaneously forming the PPy nanotubes. The influence of the concentration of Py, MO, and $FeCl_3$ were investigated to tune the diameter of PPy-NTs. Other polymerization conditions were also investigated such as temperature, reaction time and solvent types. Then the investigation focus on the influence of morphology on the capacitive behavior. By varying the different reaction conditions, maximum specific supercapacitive reaction conditions were found. The maximum specific capacitance of 960 F g^{-1} is obtained at current density 0.5 A g^{-1} with the concentrations of $FeCl_3$, MO and Py are 250 mM, 5.0 mM, and 50.0 mM, respectively.

2. EXPERIMENTAL SECTIONS

2.1 Materials

All chemicals used were of analytical grade. Pyrrole (Aladdin) was stored in a freezer. Methyl orange as a dopant was used as received. Other chemicals were used without any further purification. All aqueous solutions were prepared with freshly high purity water.

2.2 Synthesis of PPy-NTs

During the typical test, 0.243 g (1.5 mmol) of $FeCl_3$ was added in 30 mL of 5 mM MO (sodium 4-[4'-(dimethylamino) phenyldiazo] phenylsulfonate) ($(CH_3)_2NC_6H_4\text{-}N{=}NC_6H_4SO_3Na$) deionized water solution. A flocculent precipitate appeared immediately. Then 105 μL (1.5 mmol) of Py monomer was added and the mixture was stirred at room temperature for 24 h. The PPy-NTs precipitate was washed with ethanol/deionized water for several times until filtrate was neutral and colorless. The product was finally dried under a vacuum atmosphere and the temperature was keep 60 ^{o}C for 24 h. The process was repeated without the addition of MO.

2.3 Characterizations

The morphology features of the products were characterized by scanning electron microscopy (SEM) (S-4800 field emission Hitachi) and transmission electron microscopy (TEM) (Tecnai 12). energy-dispersive energy dispersive X-ray spectrometry (EDS) accessory for elemental measurement (Kevex-Sigm). The molecular structure of PPy-NTs was characterized by FT-IR spectrometer (Bruker Vector-22). A Pyris 1 TGA thermogravimetric analyzer was used to investigate the thermal stability (TGA and DTG) of the PPy with nitrogen as pure gas at a flow rate of 50 mL min^{-1} and the heating rate was keep 10 ^{o}C min^{-1}.

2.4 Electrochemical measurements

The electrochemical capacitance performance was recorded on a CHI 660D electro analysis apparatus (Shanghai Chenhua Instrument, Inc.) through cyclic voltammetry (CV) and galvanostatic charge-discharge (GCD) measurements. Electrochemical impedance spectroscopy (EIS) measurements using the electrochemical workstation (Auto Lab, Nova 1.9, Metrohm, Utrecht, The Netherlands) was conducted in a frequency range of 0.01-100000 Hz. All electrochemical performances were carried out in a three-compartment cell respectively. The three-electrode system was equipped with a platinum foil as the counter, and an Ag/AgCl electrode as the reference. The working electrode was made by mixing active materials (PPy-NTs), acetylene black, and PTFE (polytetrafluoroe-thylene) at a weight ratio of 8 : 1 : 1, coating on a piece of soft graphite of about 1 cm^2. The equipment dried under room temperature for 24 h, then pressed it to be a thin foil at the pressure of 10.0 MPa. The electrolyte was1.0 M H_2SO_4 solution.

3. RESULTS AND DISCUSSION

3.1 Characterization

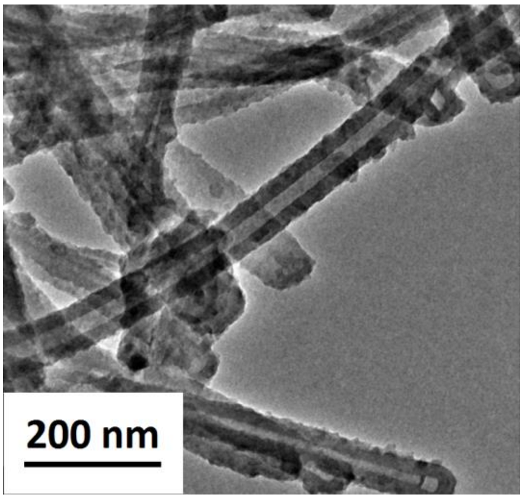

Figure 1. TEM images of PPy-NTs obtained in the presence of MO

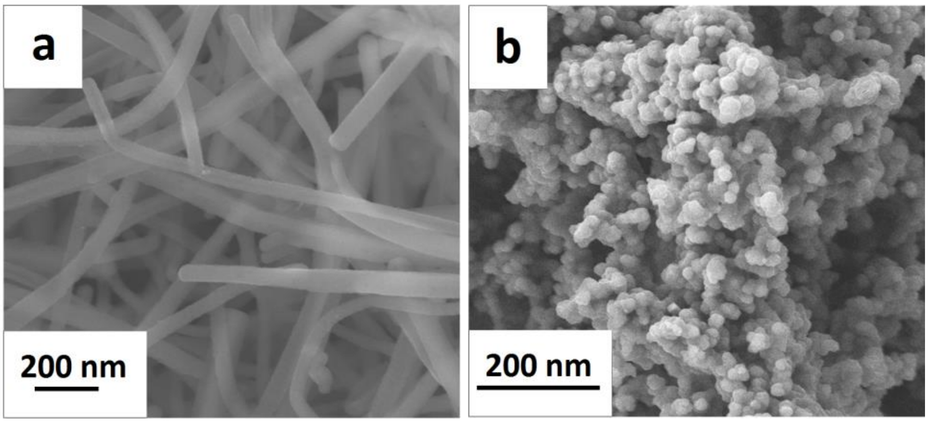

Figure 2. (a) SEM images of PPy-NTs obtained in the presence of MO; (b) SEM in the absence of MO.

As is shown in Figure 1, the PPy nanotubes were obtained in the presence of MO as the dopant. The inner and outer diameters were ~30 and ~100 nm and the nanotubes were very homogeneous from Figure2(a), respectively. While only particles were generated in the absence of MO as shown in Figure 2(b).

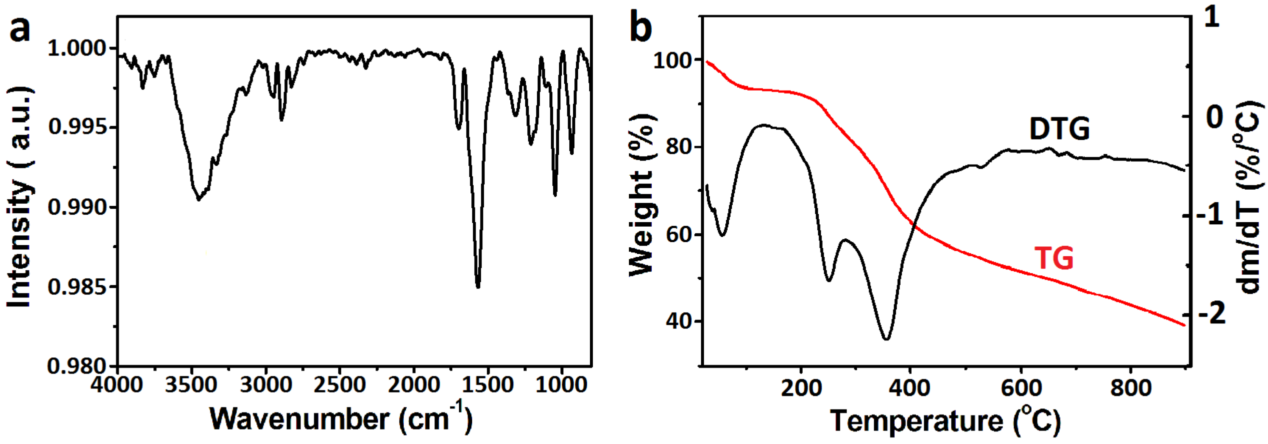

Figure 3. (a) FTIR spectrum; (b) TG and DTG curve of PPy nanotubes.

The FTIR spectrum of the PPy nanotubes was in good agreement with the previous results [36]. Characteristic peaks of PPy were observed in Figure 3(a), such as PPy-ring fundamental vibration centered at 1535 and 1459 cm^{-1}, the C–N stretching vibration at 1169 cm^{-1}, a C–H was wagging vibrations at 785 cm^{-1}, the =C–H in-plane vibration at 1302 and 1042 cm^{-1}, and the =C–H out-plane vibration at 900 cm^{-1}.

As is shown in Figure 3(b), in the range of 25 to 140 °C, the chemically prepared PPy started losing weight, which may be associated to the departure of absorbed solvent and water in the PPy powder; In the range of 140 to 280 °C, the losing weight may be associated with the departure of micro-molecule and the dopant of PPy; In the range of 280 to 580 °C, the weight loss originates from the decompose of molecular chain of polypyrrole [37].

Table 1. EDS results of PPy-NTs synthesized in the presence of MO.

Element	C	N	O	Fe	Cl	S
Content (%)	75.45	11.65	6.38	0.35	2.35	3.81

EDS analysis (Table. 1) provides the composition of PPy-MO nanotubes. It indicates that PPy-NTs was obtained in presence of MO is doped with MO, Cl, and a small amount of iron. The degree of doping of the PPy-NTs nanotube can be calculated by the formula of [MO]/[Py] which was denoted by the ratio [S]/([N]–3[S]) = 0.25. MO plays a role of not only a dopant but also a template for forming nanotubes structures [18].

3.2 Tuning the diameter of PPy nanotubes

To tune the diameter of PPy nanotubes, the polymerization parameters were varied. The temperature is an important factor for PPy nanotube polymerization, which affects the aggregation number of micelles [38]. PPy-NTs were aggregated (Figure4(a) to Figure4(e)). At the temperature of 40 ^oC, it is impossible to get the PPy nanotubes as shown in Figure 4(f).

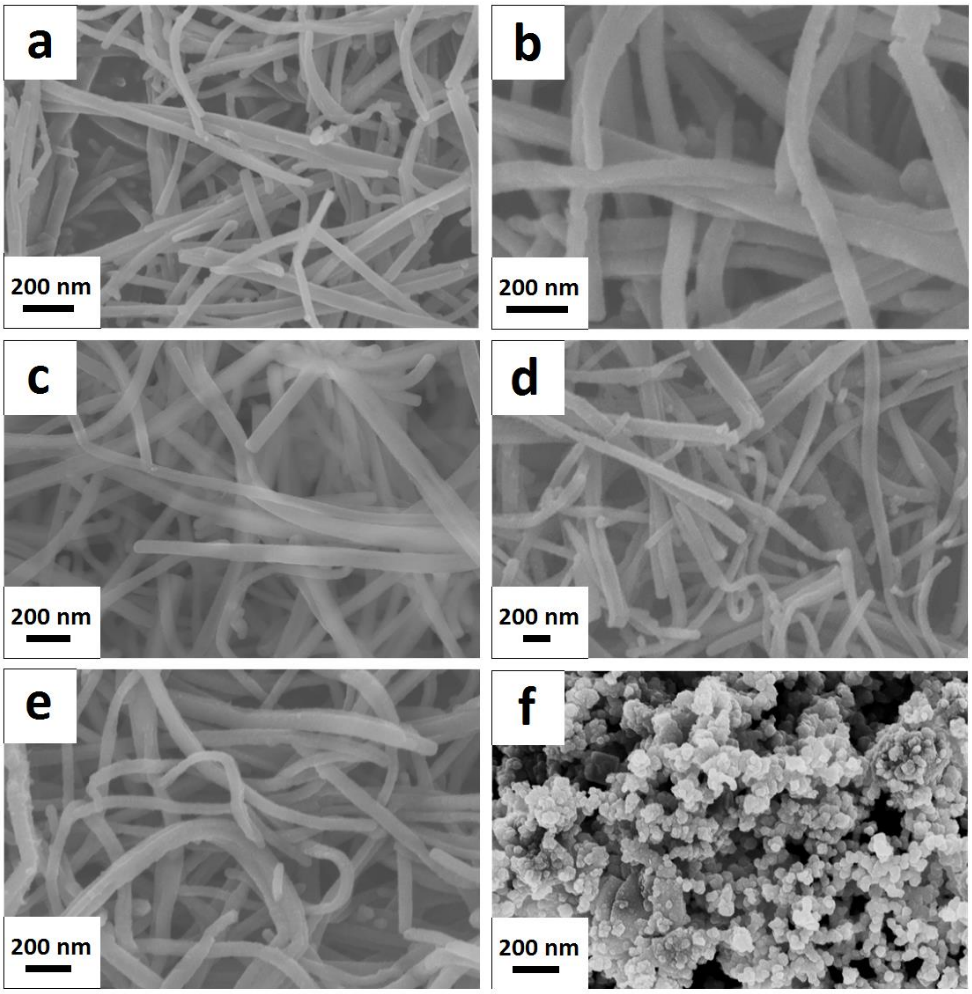

Figure 4. SEM images of PPy with different temperatures: a) 0 ^oC; b) 10 ^oC; c)15 ^oC; d) 25 ^oC; e) 30 ^oC, and f) 40 ^oC, respectively.

When the temperature was 0-30 ^oC, the dimeter has no large change. In the appropriate range of temperature, we can synthesis the PPy nanotube which has the stable diameter of 100 nm as was shown in Figure 5(a).

The concentration of Py, MO, and $FeCl_3$ is another important factor for PPy nanotube polymerization, which affects the diameter of PPy nanotubes. PPy-NTs were obtained with a relatively stable diameter which was ~100 nm under the following condition:

(1) the concentration of Py and $FeCl_3$ were constant with a value of 50.0 mM and the concentration of MO was between 2.5 and 5 mM (Figure 5(b)), When the concentration of MO was very low, the MO molecular was dissolved in water with dispersion state, and when a certain concentration was reached, aggregates are formed to form planar vesicles. Therefore, when the concentration of pyrrole and $FeCl_3$ is constant, with the increase of MO, it is beneficial to the formation of special planar vesicles during the reaction process, and PPy-NTs was obtained;

(2) The concentration of MO and $FeCl_3$ were constant with a value of 5.0 mM, and 50.0 mM and the concentration of Py was between 5 and 50 mM(Figure 5(c)), When the pyrrole concentration was less than 5 mM, the synthesized PPy-NTs was not dense enough, and granular products was appeared due to the low concentration of pyrrole monomer. The accumulation of particles leaded to an increase in diameter. When the concentration of py was above 100 mmol, the diameter of PPy-NTs increased by a certain amount. This might be that the polymerization rate increased with the increase of py concentration, PPy-NTs polymerization quickly and it leaded to an increase in diameter;

(3) The concentration of MO and Py were constant with a value of 5.0 mM, and 50.0 mM and the concentration of $FeCl_3$ was between 50 and 250 mM (Figure 5(d)).

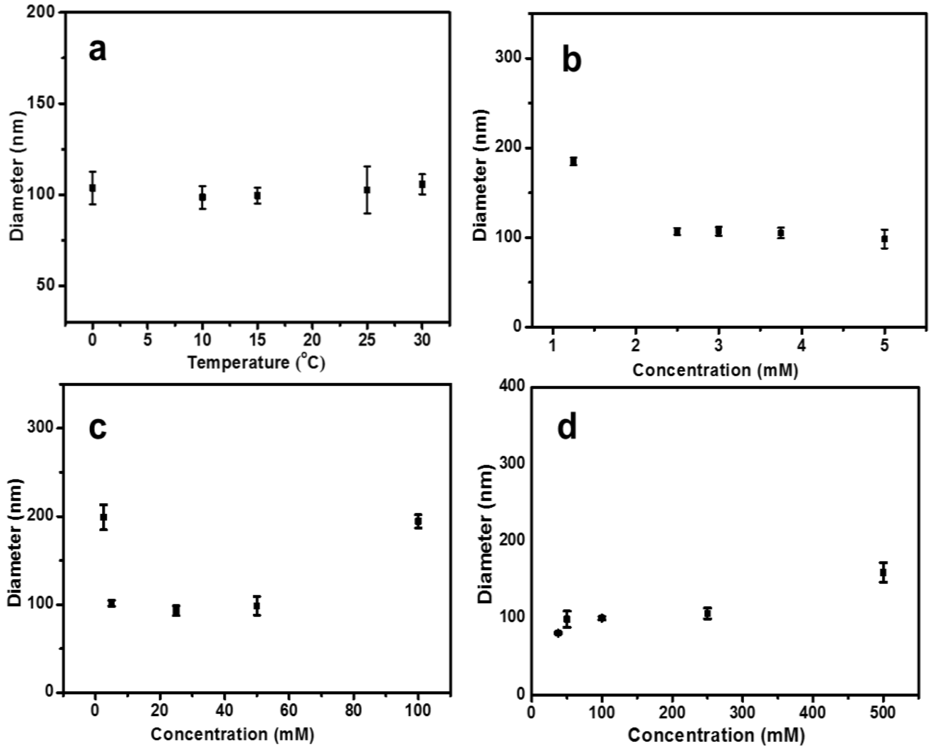

Figure 5. (a) Diameter of PPy nanotubes obtained at different temperature; Diameter of PPy nanotubes obtained at different concentration; (b) MO when the concentration of Py and $FeCl_3$ were constant with a value of 50.0 mM, (c) Py when the concentration of MO and $FeCl_3$ were constant with a value of 5.0 mM, and 50.0 mM, (d) $FeCl_3$ when the concentration of MO and Py were constant with a value of 5.0 mM, and 50.0 mM.

The addition of $FeCl_3$ was too low, could not synthesize PPy-NTs in time and the resulting nanotubes were thinner, When the concentration of $FeCl_3$ was too high, the oxidation rate become faster, the PPy-NTs could not be arranged in time, $FeCl_3$ unresponsive attached to the surface of the nanotubes, leaded to an increase in diameter.

The polymerization time was also an important factor for PPy nanotube polymerization, which affects the diameter of PPy nanotubes. At the beginning of the reaction, the diameter of the PPy nanotubes was relatively small and the morphology was non-uniform. After 1 h the diameter of the nanotubes maintains constant and the morphology become uniform as shown in Figure 6.

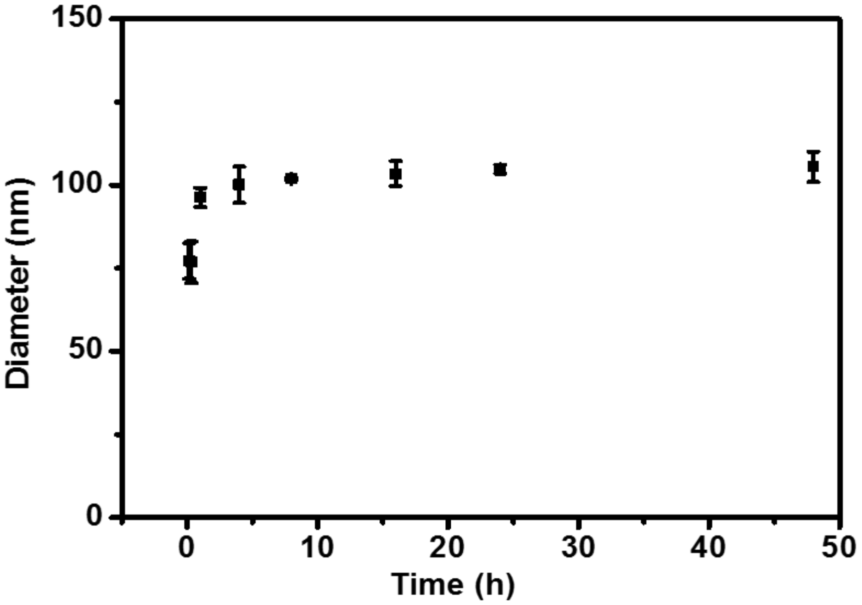

Figure 6. Diameter of PPy nanotubes obtained at different time.

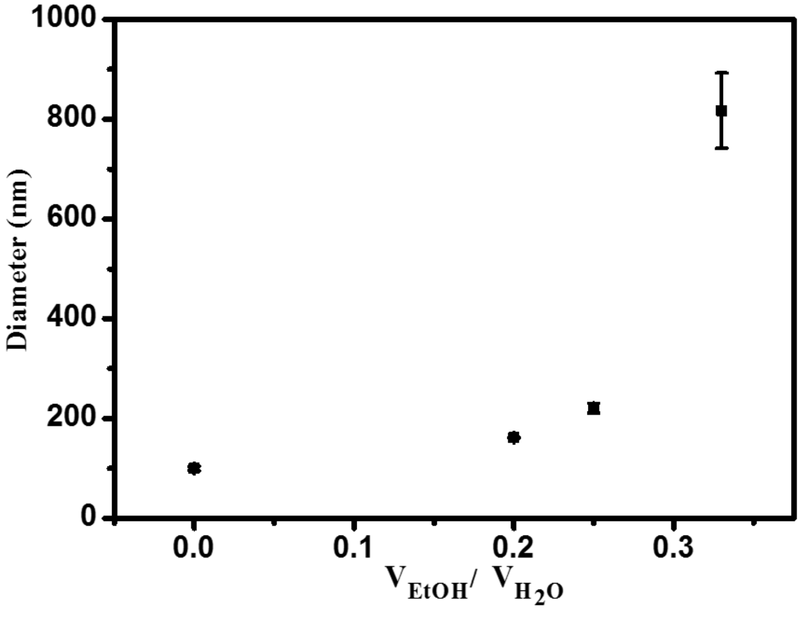

Figure 7. Dimeter of PPy nanotubes obtained at different volume ratio of ethanol and water.

The reaction solvent was also studied. As is shown in Figure 7(a), When the ratio was 0.33, the dimeter was 816 nm while it was ~100 nm when V_{EtOH}/V_{H2O} was under 0.33. There was a certain change about the length of nanotubes with different volume ratio of ethanol and water (Figure 8(a-d)). Experimental proofed that when the ratio was 0.5 we couldn't obtain nanotubes. As the proportion of ethanol decreases, the diameter becomes larger and these changes would inevitably lead to variety in electrochemical performance

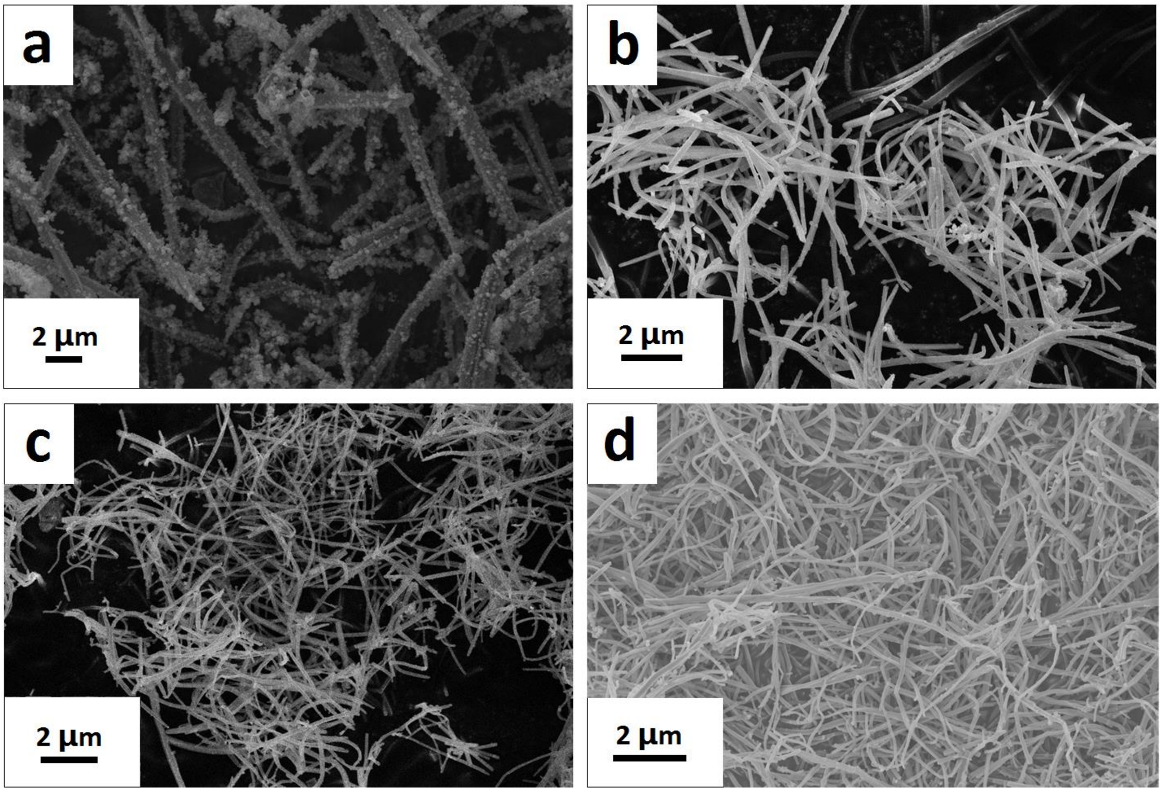

Figure 8. SEM of PPy nanotubes obtained at different volume ratio of ethanol and water, (a) V_{EtOH}/V_{H2O} =1:3; (b) V_{EtOH}/V_{H2O}=1:4; (c) V_{EtOH}/V_{H2O}=1:5;(d) V_{EtOH}/V_{H2O} =0:1.

3.3 Influence of morphology on the capacitive behavior.

The electrochemical properties of PPy-NTs electrodes were studied using CV and GCD measurements in 1 M H_2SO_4 electrolyte. The specific capacitances of PPy-NTs electrodes were calculated from the discharging curves using following equation,

$$C_s = \frac{I_d \times T_d}{\Delta V \times m}$$

where, Cs is specific capacitance, T_d is the discharge time, I_d is discharge current, ΔV is potential window, and m is the mass of active material. For PPy-NTs electrodes, the mass of active material was 1 mg/cm^{-2}.

From Figure 9(a), the specific capacitances were similar to each other of PPy-NTs obtained in the different temperature. In the investigated above, at the appropriate range of temperature, we can obtain the PPy-NTs with stable diameter of ~100 nm. The specific capacitance is related to the dimeter of PPy-NTs. The maximum specific capacitance of 552.86 F g^{-1} was obtained within potential window of 0.2-0.9 V (vs. Ag/AgCl) at 0.5 A g^{-1}.

The concentration of Py, MO, and $FeCl_3$ affects the diameter of PPy nanotubes. The specific capacitance is related to the dimeter. As is shown in Figure 9, different specific capacitance obtained by different concentration of reactants.

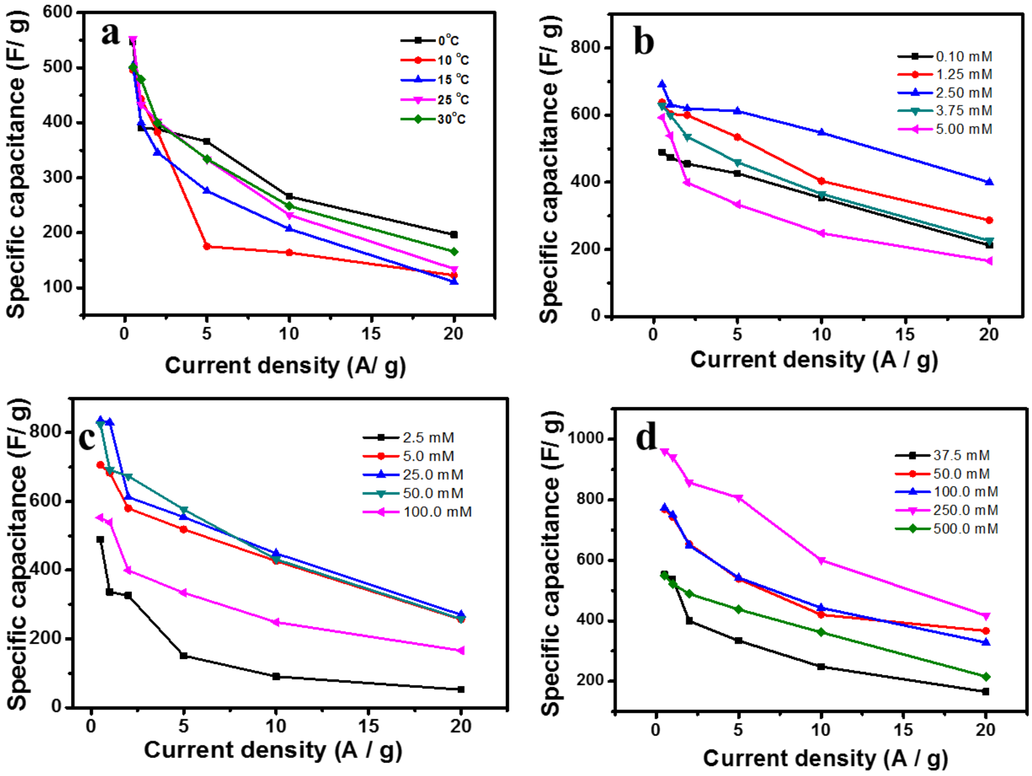

Figure 9. Specific capacitance at different current densities of PPy-NTs (a) obtained at different temperature; PPy-NTs obtained at different reactants concentration of (b) MO when the concentration of Py and $FeCl_3$ were constant with a value of 50.0 mM; (c) Py when the concentration of MO and $FeCl_3$ were constant with a value of 5.0 mM, and 50.0 mM; (d) $FeCl_3$ when the concentration of MO and Py were constant with a value of 5.0 mM, and 50.0 mM.

From Figure 9(b), the maximum specific capacitance of 691.25 F g^{-1} at 0.5 A g^{-1}within potential window of 0-0.8 V (vs. Ag/AgCl) was obtained by concentration of MO was 1.25 mM when the concentration of Py and $FeCl_3$ were constant with a value of 50.0 mM. As is shown in Figure 9(c) the maximum specific capacitance of 835 F g^{-1} at 0.5 A g^{-1} within potential window of 0.2-0.9 V (vs. Ag/AgCl) was obtained by concentration of Py 25 mM and concentration of MO and $FeCl_3$ were constant with a value of 5.0 mM, 50.0 mM; From Figure 9(d), the maximum specific capacitance of 960 F g^{-1} at 0.5 A g^{-1} within potential window of 0.2-0.8 V (vs. Ag/AgCl) was obtained by $FeCl_3$ 250 mM and the concentration of MO and Py were constant with a value of 5.0 mM, 50.0 mM. When the concentration of reactants were changed, the maximum capacitance of PPy-NTs were obtained and the diameter of the nanotubes distributed in ~100 nm. Facts proved that When the ratio of MO: Py: $FeCl_3$

was 1 : 10 : 50, the maximum specific capacitance of 960 F g^{-1} at 0.5 A g^{-1} was obtained and the diameter was ~106 nm.

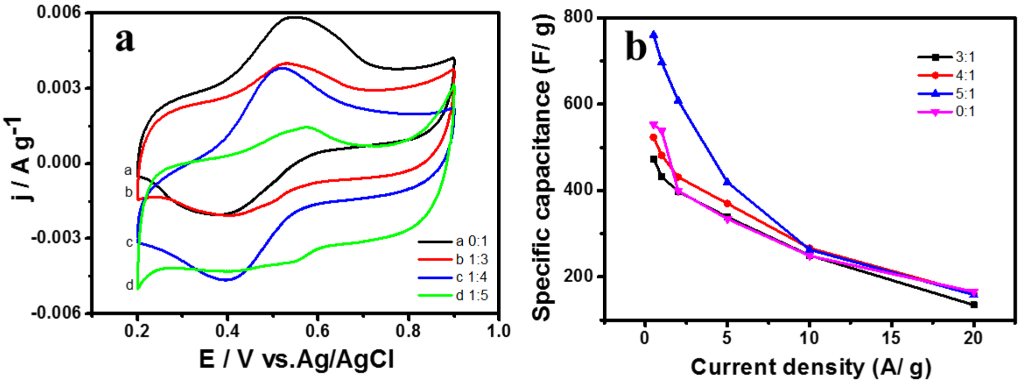

Figure 10. (a) CV curves of PPy (0.005 V/s), (b) Polt of specific capacitance at different current densities for PPy nanotubes obtained at different volume ratio of ethanol and water.

Figure 10(a), All samples showed significant redox peaks and it was shown that the PPy-NTs exhibits a typical pseudo-capacitance characteristic. Dimeter was affected by the type of solvent. Different volume ratio of ethanol and water. When the ratio was 0.33, the dimeter became ~ 816 nm and specific capacitance is 494.29 F g^{-1} at 0.5 A g^{-1} from Figure 10. As the diameter increases, the specific capacitance relatively reduces because of the decrease of relative specific surface area. The specific capacitance is 760.71 F g^{-1} at 0.5 A g^{-1} when the ratio of ethanol and water was 0.2 (Figure 10(b)).

Table 2. Capacitance properties of some recently published PPy-based electrode materials.

Material	Specific capacitance (F g^{-1}) (low current density/scan rate)	Specific capacitance (F g^{-1}) (high current density/scan rate)	Capacity retention (%)
Polypyrrole nanowires [6]	420 (1.5 A g^{-1})	272 (18 A g^{-1})	97.9% (8000 cycles, 1.5 A g^{-1})
Porous polypyrrole clusters [42]	586 (2 mV s^{-1})	—	—
Polypyrrole Film [43]	—	261 (25 mV s^{-1})	75% (1000 cycles, 25 mV s^{-1})
Polypyrrole Film [44]	254 (2 mV s^{-1})	—	—
Polypyrrole Film [45]	403 (0.5 mA cm^{-2})	360 (5 mA cm^{-2})	—
Polypyrrole Film [46]	406 (5 mV s^{-1})	260 (1000 mV s^{-1})	92.6% (50000 cycles, 50 A g^{-1})
Polypyrrole nanoplates [47]	533 (5 mV s^{-1})	412 (100 mV s^{-1})	78% (5000 cycles, 100 mV s^{-1})
Polypyrrole nanotubes (This work)	960 (0.5 A g^{-1})	426 (20 A g^{-1})	97.1% (10000 cycles, 0.5 A g^{-1})

Figure 11(a) and Figure 11(b) were the CV curves and GCD curves for the PPy-NTs obtained at the concentration of $FeCl_3$ was 250 mM when the concentration of MO and Py were constant with a value of 5.0 mM, and 50.0 mM. As is shown in Figure 11(a) PPy-NTs at varied scan rates in a voltage range between 0.2 and 0.8 V (vs. Ag/Ag Cl). The CV curves show obvious well-defined redox peaks and still well retained for PPy-NTs electrodes, presenting the main capacitive behavior from pseudo-capacitance of PPy. The mass for PPy-NTs electrodes of active material was keep 1 mg/cm^{-2}. The maximum specific capacitance of 960 F g^{-1} is obtained at current density 0.5 A g^{-1} for PPy-NTs electrode from Figure 11(b). When the current density is increased to 20 A g^{-1}, the specific capacitance still maintain 426 F g^{-1}. Figure 11(c) shows the electrochemical stability of PPy-NTs electrodes at a current density of 0.5 A g^{-1}. Until 10000 cycles, the capacitance of PPy-NTs electrodes remain stable afterward and the final specific capacitance retention rate are almost about 97.1%. A comparison of capacitance properties that was studied in a three-electrode system between some recently published PPy-based electrode materials and this work is given in Table 2.

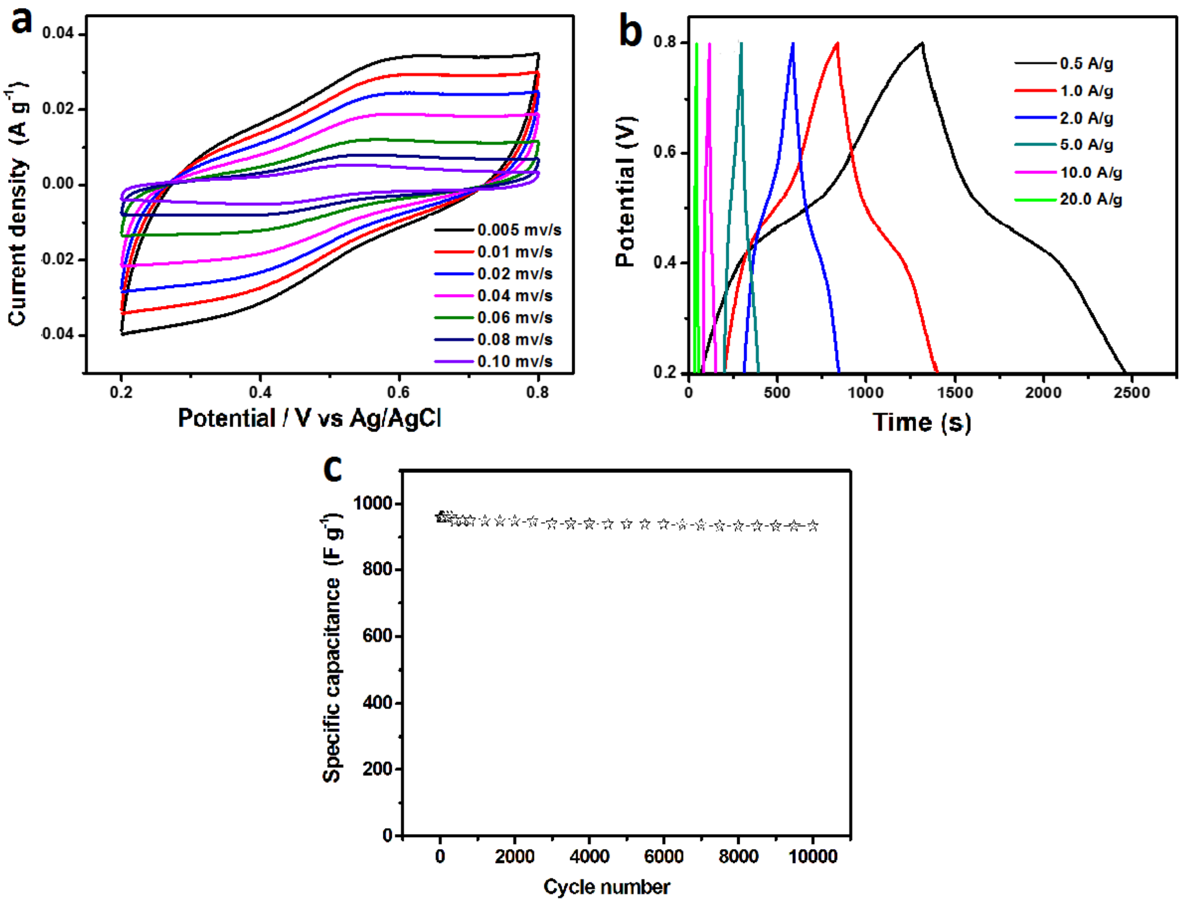

Figure 11. (a) CV curves within a range 0.2-0.8 V; (b) Galvanostatic charge-discharge curves of PPy-NTs active materials; (c) Cyclic performance of PPy-NTs active materials electrode measured at a constant current density of 0.5 A g^{-1}.

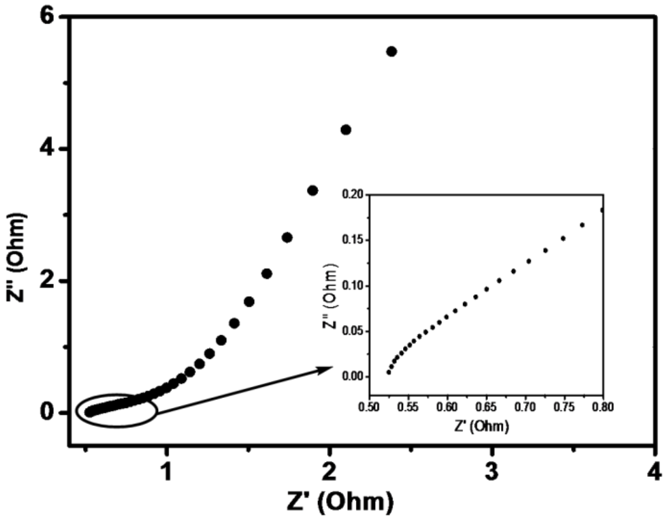

Figure 12. EIS Nyquist polt of PPy-NTs obtained by $FeCl_3$ 250 mM and the concentration of MO and Py were constant with a value of 5.0 mM and 50.0 mM in solution of 1 M H_2SO_4 (The insert show the enlarged Nyquist polt at high frequency region)

The EIS in the frequency range of 0.01 Hz to 105 Hz was conducted on PPy-NTs to understand the charge transfer of PPy-NTs electrode material (Figure 12(c)). The ion diffusion of electrolyte was also conducted by EIS graphics. Figure 12(c) shows the EIS Nyquist plots vs. Ag/AgCl in the 1 M H_2SO_4 electrolyte solution. The ohmic resistance could be evaluated by real part of impedance high frequency intercept of the semicircle. The process was controlled by diffusion if the beeline showed a slope of 45^{o} at low frequency region, it was purely capacitive behavior if the slope was 90^{o} in nature. The impedance map exhibits a negligible semi-circular shape, showing a very efficient charge transfer. Obviously, the PPy-NTs electrodes presented the supercapacitive characteristic because it was composed of a straight line at low frequency range.

4. CONCLUSIONS

In summary, we have prepared the PPy-NTs by using a soluble MO template in neutral aqueous solutions. The diameter of the PPy-NTs could be tuned by changing the temperature, concentration of MO, $FeCl_3$, and Py, the ratio of the $EtOH/H_2O$. By varying the different reaction conditions, PPy-NTs with diameter of ~100 nm was obtained and maximum specific supercapacitive reaction conditions were found. The maximum specific capacitance was 960 F g^{-1} at 0.5 A g^{-1} with the concentrations of $FeCl_3$, MO and Py are 250 mM, 5.0 mM, and 50.0 mM, respectively (MO : Py : $FeCl_3$ = 1 : 10 : 50). At the same time, it also shows excellent cycle performance, after 10000 charge and discharge cycle the specific capacitance is still maintained as the original 97.1%. Accordingly, PPy-NTs could be well used as good electrode material to produce the advanced supercapacitors, The PPy-NTs exhibit high capacitance performance in energy storage devices that also can be used in the electronics industry. Future investigations will aim to solve the problem of finding the formation mechanism for forming a nanotubes structure via MO as the dopant and improving capacitance performance of PPy-NTs.

ACKNOWLEDGEMENTS
This work was supported by the Program for New Century Excellent Talents of the University in China (NCET-13-0645), the National Natural Science Foundation of China (NSFC-21201010, 21671170 and 21673203), the Natural Science Foundation of the Jiangsu Higher Education Institutions of China (No. 15KJB430034), Innovation Scientists and Technicians Troop Construction Projects of Henan Province (164200510018), Program for Innovative Research Team (in Science and Technology) in University of Henan Province (14IRTSTHN004), the Six Talent Plan (2015-XCL-030), Qinglan Project and Excellent Doctoral Dissertation of Yangzhou University. We also acknowledge the Priority Academic Program Development of Jiangsu Higher Education Institutions and the technical support we received at the Testing Center of Yangzhou University.

References

1. L. Fan, L. Tang, H. Gong, Z. Yao and R. Guo, *J. Mater. Chem.*, 22 (2012) 16376.
2. J. Tong, H. Zhang, J. Gu, L. Li, C. Ma, J. Zhao and C. Wang, *J. Mater. Sci.*, 51 (2016) 1966.
3. H. Zhang, Y. Wang, C. Liu and H. Jiang, *J. Alloys Compd.*, 517 (2012) 1.
4. Q. Wu, M. Chen, K. Chen, S. Wang, C. Wang and G. Diao, *J. Mater. Sci.*, 51(2016) 1572.
5. Y. Yan, P. Gu, S. Zheng, M. Zheng, H. Pang and H. Xue, *J. Mater. Chem. A*, 4 (2016) 19078.
6. J. Zhao, J. Wu, B. Li, W. Du, Q. Huang, M. Zheng, H. Xue and H. Pang, Prog. *Nat. Sci-Mater.*, 26 (2016) 237.
7. C. Chiang, Y. Park, A. Heeger, H. Shirakawa, E. Louis and A. Macdiarmid, *J. Chem. Phys.*, 69 (1978) 5098.
8. L. Qin, X. Zhao, K. Hirahara, Y. Miyamoto, Y. Ando and S. Iijima, *Nature*, 408 (2000)50.
9. H. Shirakawa, *Abs. Pap. ACS*, 222 (2001) U276.
10. M. Galvin and G. Wnek, *Polymer*, 23 (1982) 795.
11. C. Zhou, X. Gong, J. Han and R. Guo, *New J. Chem.*, 39 (2015) 2202.
12. J. Han, J. Dai, C. Zhou and R. Guo, *Polym. Chem.*, 4 (2013) 313.
13. A. Diaz, K. Kanazawa and G. Gardini, J. Chem. Soc. *Chem. Commun.*, 14 (1979) 635.
14. G. Song, L. Liu, J. Han, C. Wang and G. Wang, *Synthetic Met.*, 197 (2014) 126
15. G. Tourillon and F. Garnier, *J. Electroanal. Chem.*, 135 (1982) 173.
16. X. Shu, Z. Li and J. Xia, *Prog. Chem.*, 27 (2015) 385.
17. J. Xia, N. Masaki, K. Jiang and S. Yanagida, *J. Mater. Chem.*, 17 (2007) 2845.
18. R. Ramya, R. Sivasubramanian and M. V. Sangaranarayanan, *Electrochim. Acta*, 101(2013) 109.
19. J. Han, L. Li, P. Fang and R. Guo, *J. Phys. Chem. C*, 116 (2012) 15900.
20. Y. Xie and D. Wang, *J. Alloy and Compd.*, 665 (2016) 323.
21. C. Pratt, *Conducting Polymers*, (2008) 225.
22. A. MacDiarmid, *Angew. Chem. Int. Edit.*, 40 (2001) 2581.
23. X. Yang, T. Dai, Z. Zhu and Y. Lu, *Polymer*, 48 (2007) 4021.
24. X. Yang, Z. Zhu, T. Dai and Y. Lu, *Macromol. Rapid Commun.*, 26 (2005) 1736.
25. Y. Yang and M. Wan, *J. Mater. Chem.*, 11 (2001) 2022.
26. M. Zhou and J. Heinze, *J. Phys. Chem. B*, 103 (1999) 8443.
27. C. Jerome, D. Labaye and R. Jerome, *Synthetic Met.*, 142 (2004) 207.
28. M. Li, W. Li, J. Liu and J. Yao, *J. Mater. Sci.*, 24 (2013) 906.
29. Z. Zhu, Nanjing university, Master’s Thesis (2004).
30. J. Kopecka, D. Kopecky, M. Vrnata, P. Fitl, J. Stejskal, M. Trchova, P. Bober, Z. Moravkova and J.

Prokes,I. Sapurina, *Rsc Adv.*, 4 (2014) 1551.
31. V. P. Menon, A. Junting Lei and C. R. Martin, *Chem. Mater.*, 8 (1996) 2382.
32. B. Schulz, I. Orgzall, I. Díez, B. Dietzel and K. Tauer, *Colloids Surfaces A*, 354 (2010) 368.
33. Y. Li, Y. Jiang, S. Hu, X. Zhang, J. Zhai, H. Han, D. Xiao and P. Liu, *High Perform. Polym.*, 28 (2016) 225.
34. J. Jang and H. Yoon, *Langmuir*, 21 (2005) 11484.
35. M. Joulazadeh and A. H. Navarchian, *Synthetic Met.*, 199 (2015) 37.
36. Ishpal and A. Kaur, *J. Appl. Phys.*, 113 (2013) 094504.
37. M. Wei and Y. Lu, *Synthetic Met.*, 159 (2009) 1061.
38. Y. Yang, J. Liu and M. Wan, *Nanotechnology*, 13 (2002) 771.
39. J. Stejskal, I. Sapurina and M. Trchová, *Prog. Polym. Sci.*, 35 (2010) 1420.
40. J. Huang and M. Wan, J. Polym. *Sci. Pol. Chem.*, 37 (1999) 1277.
41. Y. Li, G. Li, H. Peng and K. Chen, *Polym. Int.*, 60 (2011) 647.
42. D. P. Dubal, S. H. Lee, J. G. Kim, W. B. Kim and C. D. Lokhande, *J. Mater. Chem.*, 22 (2012) 3044.
43. Q. Yang, Z. Hou and T. Huang, *J. Appl. Polym. Sci.*, 11 (2015) 132.
44. C. Shi and I. Zhitomirsky, *Nanoscale Res. Lett.*, 5 (2010) 518.
45. J. Zhang, L. B. Kong, H. Li, Y. C. Luo and L. Kang, *J. Mater. Sci.*, 45 (2010) 1947.
46. X. Du, X. Hao, Z. Wang, X. Ma, G. Guan, A. Abuliti, G. Ma and S. Liu. *Synthetic Met.*, 175 (2013) 138.
47. D. P. Dubal, S. V. Patil, A. D. Jagadale and C. D. Lokhande, *J. Alloys Compd.*, 509 (2012) 8183.